

A self-consistent value of the electric radius of the proton from the Lamb shift in muonic hydrogen

Savely G. Karshenboim*

*Max-Planck-Institut für Quantenoptik, Garching, 85748, Germany and
Pulkovo Observatory, St.Petersburg, 196140, Russia*

Recently a high-precision measurement of the Lamb shift in muonic hydrogen has been performed. An accurate value of the proton charge radius can be extracted from this datum with a high accuracy. To do that a sufficient accuracy should be achieved also on the theoretical side, including an appropriate treatment of higher-order proton-structure effects. Here we consider a higher-order contribution of the finite size of the proton to the Lamb shift in muonic hydrogen. Only model-dependent results for this correction have been known up to date. Meantime, the involved models are not consistent either with the existing experimental data on the electron-proton scattering or with the value for the electric charge radius of the proton extracted from the Lamb shift in muonic hydrogen. We consider the higher-order contribution of the proton finite size in a model-independent way and eventually derive a self-consistent value of the electric radius of the proton. The re-evaluated value of the proton charge radius is found to be $R_E = 0.840\,22(56)$ fm.

PACS numbers: 12.20.-m, 13.40.Gp, 31.30.J-, 36.10.Gv

I. INTRODUCTION

There is a controversy in a determination of the electric charge radius of the proton. The most accurate value (as claimed) of the proton charge radius comes from the measurements of the Lamb shift in muonic hydrogen by the CREMA collaboration [1, 2]. It strongly disagrees with the scattering results [3, 4] (as well as with the result from hydrogen and deuterium spectroscopy summarized in [5]). The situation is summarized in Fig. 1 where two basic scattering results are presented. Sick [3] has evaluated all the world data, but MAMI results [4]. Other evaluations without MAMI data produced similar results. MAMI results are presented in the plot separately.

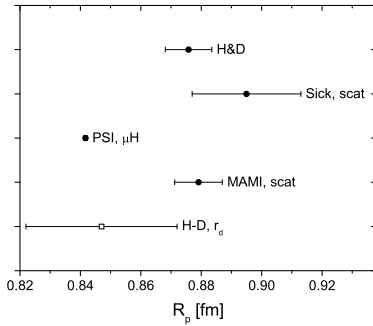


FIG. 1: Determination of the rms proton charge radius. For details see [6, 7].

Meantime, to extract the value of the proton radius from the μ H Lamb shift one has to integrate the proton

form factor over a broad area in momentum space with a contribution from the low momenta being enhanced.

A straightforward evaluation based on fitting of scattering data is not appropriate since the results of such a fitting are not consistent with the results on the muonic hydrogen Lamb shift.

Alternatively, one may use a certain model, such as the dipole parametrization. Its parameter has to be related to the proton radius. That makes the form factor incompatible with the scattering data. (As it is well known, the dipole parametrization is consistent with the higher-momentum transfer data with the parameter inconsistent with any radius in Fig. 1.)

Apparently, both these options are not satisfactory. However, up to date only such evaluations have been performed to extract the proton radius from the muonic hydrogen (see, e.g., [1, 2]).

The μ H result for the proton radius was obtained for the first time in [1]. The theoretical expression for the Lamb shift was presented there as

$$E(2p_{1/2} - 2s_{1/2}) = (206.0573(45)_{\text{QED}} - 5.2262r_p^2 + 0.0347r_p^3) \text{ meV}, \quad (1)$$

where $r_p = R_E/\text{fm}$ is the numerical value of the proton charge radius in the units of Fermi (= femtometer). The term denoted here as ‘QED’ is dominated by the QED contributions, but contains also some non-QED terms such as the proton polarizability contribution.

Consider this expression in detail. In the model-independent terms, one has to write rather

$$E(2p_{1/2} - 2s_{1/2}) = (206.0573(45)_{\text{QED}} - 5.2262r_p^2) \text{ meV} + \frac{2(Z\alpha)^5 m_r^4}{\pi} I_3^E, \quad (2)$$

*Electronic address: savely.karshenboim@mpq.mpg.de

where m_r is the reduced mass. Here¹

$$I_3^E \equiv \int_0^\infty \frac{dq}{q^4} \left[(G_E(q^2))^2 - 1 - 2G'_E(0)q^2 \right], \quad (3)$$

is the integral we are interested in this paper. It describes the next-to-leading higher-order proton-finite-size contribution to the μH Lamb shift. (The related contribution to the Lamb shift in ordinary hydrogen is negligible.) We use the relativistic units in which $\hbar = c = 1$ throughout the paper.

The representation (1), applied in [1], was obtained (see, e.g., [8]) within the dipole parametrization

$$G_{\text{dip}}(q^2) = \left(\frac{\Lambda^2}{q^2 + \Lambda^2} \right)^2,$$

which describes the whole electric form factor with a single parameter adjusted there to the value of the proton charge radius. As it is well known, such a parametrization with $\Lambda^2 = 0.71 \text{ GeV}^2$ is a good one at higher momentum, but it produces the radius which agrees neither with the proton-scattering evaluation nor with the result from muonic hydrogen. Meanwhile, while using a parameter consistent with the muonic-hydrogen Lamb shift [1], the dipole parametrization is not consistent with the experimental scattering data any more. In other words, the low-momentum behavior of the form factor, established through the measurement [1], and its high-momentum behavior, established by scattering data, cannot be successfully described by the dipole parametrization with a single parameter.

Actually, there is no parametrization of the proton form factor which is literally correct and consistent with the data. Most of the empiric parametrizations [9–13] (see Appendix A for detail) deal with the ratio of polynomials in q^2 . (Here, q is the Euclidean momentum and negative values of q^2 represent the time-like region.) It is known that the form factor should have a cut line at negative q^2 starting from $4m_\pi^2$. Meantime a rational parametrization can produce only [a few] poles, but no branch point. There is no uncertainty assigned to such a mismatch. (There is a number of fits with even worse analytic behavior or with wrong asymptotic behavior at high q^2 .) Meantime, any efforts to produce a theoretically motivated parametrization with a correct position of the cut line and a correct discontinuity function on the cut line (see, e.g., [14]) are far from good agreement with the experimental data (if we rely on the χ^2 criterion).

Below we look for a realistic estimation of the uncertainty in the calculation of I_3^E and a self-consistent determination of R_E from muonic hydrogen.

¹ The other notation used is

$$\langle r^3 \rangle_2 = \frac{48}{\pi} I_3^E.$$

The names are *the Friar momentum* or *the third Zemach momentum*.

To calculate the integral I_3^E in (3), we have to integrate over the subtracted form factor,

$$(G_E(q^2))^2 - 1 - 2G'_E(0)q^2.$$

Obviously, we have no direct experimental knowledge of it both at low and high momenta. All that was used previously by various authors as the integrand was a result of fitting rather than direct measurements.

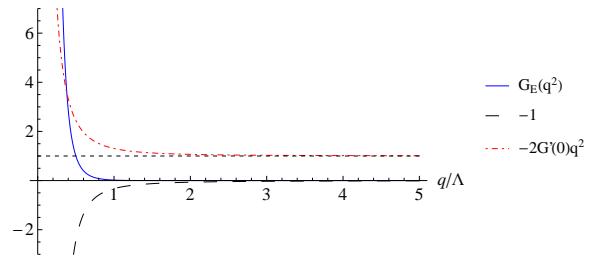


FIG. 2: Fractional contributions to the integrand in (3) as a function of q/Λ as follows from the dipole model. The red dot-dashed line is for the subtraction term with $G'_E(0)$. The dashed line is for the subtraction term with 1 and the blue solid line is for the G_E^2 term, which should follow the experimental data.

The situation for an integration over experimental data is illustrated in Fig. 2. We use there the dipole parametrization to roughly estimate the scale of contributions of separate terms. Various fractional contributions to the integrand are presented as a function of q/Λ . The red dot-dashed line is for the subtraction term with $G'_E(0)$, which is determined from a fit and is to be directly related to R_E^2 . The blue solid line is for the G_E^2 term. This term should be determined by the experimental data. The integral is fast convergent with high q . Above $q = 0.6\Lambda$ the red dot-dashed line, which is determined completely by the fit at zero momentum, is the absolutely dominant contribution. Meanwhile at low q separate contributions are divergent and only their strong cancellation, which can be successfully done only within a model, makes the integral convergent.

We are going to split the integration into two parts:

$$I = \int_0^\infty dq \dots \equiv I_{<} + I_{>} \equiv \int_0^{q_0} dq \dots + \int_{q_0}^\infty dq \dots \quad (4)$$

which are to be treated differently. (We in part explore here an idea suggested earlier in [15] for a somewhat similar integral for the hyperfine splitting in hydrogen.)

At higher momenta, we will use ‘direct’ experimental data. (We put ‘direct’ into the quotation marks because we rather intend to apply in a certain way various appropriate empiric fits than the data themselves.) The accuracy of the form factors is roughly 1%. Once one uses the ‘direct data’ the integral $I_{>}$ is indeed not really convergent at $q_0 \rightarrow 0$, because the experimental value of

$G_E(0)$ (or at any q closely approaching to zero) is not equal to unity — it is only consistent with unity within the uncertainty. The smaller is q_0 , the larger is the uncertainty of the related integral. It becomes divergent at $q_0 \rightarrow 0$, unless one substitutes the data by a fit, which we are not going to do in the low-momentum area.

Beside the integration over the data, there are also two subtraction terms (see Fig. 2). One of them does not depend on the fit and the data (it is related to the unity in the numerator in (3)) and the other, which is proportional to $G'_E(0)$, is presented in terms of the electric charge radius

$$G'_E(0) = -\frac{1}{6}R_E^2,$$

which is not a parameter to be found from the fit of the scattering data, but a constant to be determined from the eventual evaluation of the Lamb shift in muonic hydrogen.

Thus we arrive at

$$I_{3>}^E \equiv I_{3>}^E(\text{data}) + \frac{1}{3}R_E^2 \int_{q_0}^{\infty} \frac{dq}{q^2}. \quad (5)$$

On the other hand, we can take advantage of expanding the form factor at low momenta

$$(G_E(q^2))^2 = A + Bq^2 + Cq^4 + \dots \quad (6)$$

Some contributions into

$$I_{3<}^E \equiv \int_0^{q_0} \frac{dq}{q^4} \left[(G_E(q^2))^2 - 1 - 2G'_E(0)q^2 \right],$$

vanish because of the subtraction and the uncertainty comes from the remaining terms. The smaller is q_0 , the smaller is the uncertainty. One finds $A = 1$ and $B = -R_E^2/3$, with the A and B terms canceling out. The leading non-vanishing term is the C term, which is now responsible for the contribution and the uncertainty of the integration over the low momenta.

The idea is to apply a certain model to estimate the uncertainties and to find an optimal value of q_0 which corresponds to the smallest uncertainty possible. Afterwards, we can apply a more sophisticated description of the data and to find the related part of $I_{>}$ by integrating over them.

As for the model to estimate the uncertainty, we note that the dipole form factor provides a reasonable estimation for the form factor as far as we discuss general features, but not any accurate particular value. So, we can, e.g., set for (6)

$$C = C^{\text{dip}} \times (1 \pm 1),$$

where C^{dip} is the dipole value.

The details of the estimation (whether, e.g., it should be 0 ± 1 , 1 ± 0.5 , or 0.5 ± 1) may be discussed separately. C is here the curvature of the $(G_E(q^2))^2$ curve and thus

it is a certain general feature, which we expect, is reasonably good presented by the dipole approximation. One may expect that the dipole fit follows from the dispersion relations as a simplified model for the dispersion density and thus reflects physics (within certain margins).

II. CONSIDERATION WITHIN THE STANDARD DIPOLE MODEL

First, let us calculate the integral within the standard dipole approximation, the result of which is indeed well known (see, e.g. [8]):

$$\begin{aligned} I_3^{\text{dip}} &= \int_0^{\infty} \frac{dq}{q^4} \left[(G_{\text{dip}}(q^2))^2 - 1 - 2G'_{\text{dip}}(0)q^2 \right] \\ &= \frac{105}{32} \frac{\pi}{\Lambda^3} \\ &\simeq 17.2 \text{ GeV}^{-3} \\ &\simeq 0.132 \text{ fm}^3. \end{aligned} \quad (7)$$

For numerical evaluations we use $\Lambda^2 = 0.71 \text{ GeV}^2/c^2$ ($\Lambda = 0.843 \text{ GeV}$). We also remind that

$$R_{\text{dip}}^2 = \frac{12}{\Lambda^2}.$$

The value related to $\Lambda^2 = 0.71 \text{ GeV}^2/c^2$ is 0.811 fm , which is indeed too low to be correct (cf. Fig. 1).

III. SPLITTING THE INTEGRAL INTO PARTS

The dipole fit is a good first approximation for a central value of the form factor. The question is the accuracy. We assume that we know the form factor for all areas of interest with accuracy at the level of 1%. That is indeed not sufficient to calculate the integral (3) directly, but it can be applied for estimation of the uncertainty of $I_{>}$ and eventually to find an optimal value of the separation parameter q_0 , which minimizes the total uncertainty.

Let us start with $I_{>}$

$$\begin{aligned} I_{3>}^E &= \int_{q_0}^{\infty} \frac{dq}{q^4} \left[(G_E(q^2))^2 - 1 - 2G'_E(0)q^2 \right] \\ &= \int_{q_0}^{\infty} \frac{dq}{q^4} (G_E(q^2))^2 - \frac{1}{3q_0^3} - \frac{2G'_E(0)}{q_0}. \end{aligned} \quad (8)$$

The uncertainty comes from the first term only. The subtractions do not contribute to the uncertainty as far as the third term with $G'_E(0)$ is considered separately as in (5) (see below).

Thus to estimate the uncertainty we arrive at

$$\begin{aligned}
\delta I_{3>}^E &= \delta \int_{q_0}^{\infty} \frac{dq}{q^4} (G_E(q^2))^2 \\
&\simeq \delta \int_{q_0}^{\infty} \frac{dq}{q^4} (G_E(q_0^2))^2 \\
&\simeq \frac{1}{3(\nu\Lambda)^3} \frac{2\delta G_E(q_0^2)}{G_E(q_0^2)} (G_d(q_0^2))^2 \\
&= \frac{1}{3(\nu\Lambda)^3} \frac{2\delta G_E(q_0)}{G_E(q_0^2)} \left(\frac{1}{1+\nu^2} \right)^4. \quad (9)
\end{aligned}$$

where

$$\nu = \frac{q_0}{\Lambda}.$$

Here, we suggest that the uncertainty comes only from integration around the lower limit, where the form factor can be roughly estimated by the dipole fit.

To better understand a possible outcome qualitatively, it is useful to consider rather relative contributions than the absolute ones. Since the exact value used for the normalization does not play any real role here, we apply the dipole value (7) of I_3 for this purpose. In particular, assuming that we experimentally know the form factor within 1% uncertainty, we find

$$\frac{\delta I_{3>}^E}{I_3^E} \simeq \frac{0.00065}{\nu^3} \left(\frac{1}{1+\nu^2} \right)^4. \quad (10)$$

As we mention above, the $G'(0)$ contribution needs a specific treatment. That contribution

$$\begin{aligned}
I_3^R &\equiv \int_{q_0}^{\infty} \frac{dq}{q^4} [-2G'_E(0)q^2] \\
&= \frac{1}{3} \int_{q_0}^{\infty} \frac{dq}{q^2} R_E^2 \\
&= \frac{1}{3} \frac{R_E^2}{q_0} \quad (11)
\end{aligned}$$

should ‘renormalize’ the r_p^2 coefficient in the theoretical expression, which now reads as

$$\begin{aligned}
E(2p_{1/2} - 2s_{1/2}) &= (209.9779(45)_{\text{QED}} - 5.2226r_p^2) \text{ meV} \\
&+ \frac{2(Z\alpha)^5 m_r^4}{3\pi} \frac{R_E^2}{q_0} \\
&+ \frac{2(Z\alpha)^5 m_r^4}{\pi} (I_3^E - I_3^R). \quad (12)
\end{aligned}$$

Now, let us consider $I_{3<}$. At low q^2 we find for G_{dip}^2

$$\left(\frac{\Lambda^2}{\Lambda^2 + q^2} \right)^4 = 1 - 4\frac{q^2}{\Lambda^2} + 10\left(\frac{q^2}{\Lambda^2}\right)^2 - 20\left(\frac{q^2}{\Lambda^2}\right)^3 + \dots$$

and we suggest for the ‘real’ form factor

$$(G_E(q_0^2))^2 = 1 - 4a\frac{q^2}{\Lambda^2} + 10b\left(\frac{q^2}{\Lambda^2}\right)^2 \quad (13)$$

the coefficients a and b are not too far from the unity. We are to set here $b = 1 \pm 1$. We denote ± 1 as $\pm\delta b$.

So, we find

$$\begin{aligned}
I_{3<}^E &\simeq 10b \int_0^{q_0} \frac{dq}{\Lambda^4} \\
&= 10(1 \pm \delta b) \frac{\nu}{\Lambda^3} \quad (14)
\end{aligned}$$

and

$$\frac{\delta I_{3<}^E}{I_3^E} \simeq 0.97 \delta b \nu. \quad (15)$$

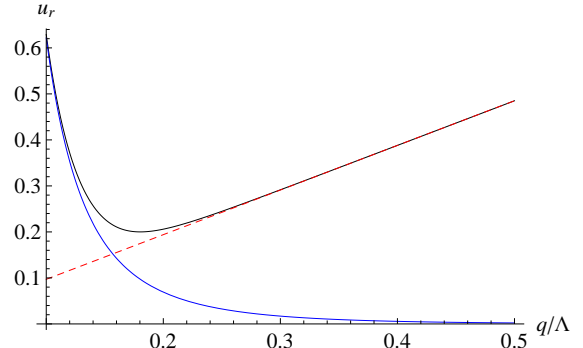


FIG. 3: The final relative uncertainty as the rms sum of contributions of (10) and (15) plotted as a function of $\nu = q_0/\Lambda$. The partial uncertainties (10) and (15) for $I_{3>}$ and $I_{3<}$ are also presented. The red dashed line is for $\delta I_{3<}$ and the blue solid line is for $\delta I_{3>}$. The relative uncertainties are estimated assuming that the central value is determined by the standard dipole fit.

Finally, we obtain

$$\frac{\delta I_3^E}{I_3^E} \simeq 20\%$$

at $q_0 \simeq 0.1803 \Lambda = 0.152 \text{ GeV}/c$ which is (approximately) the best choice (see Fig. 3 and Table I).

contribution	$\delta I_{3<}^E/I_3^{\text{dip}}$	$\delta(I_{3>}^E - I_3^R)/I_3^{\text{dip}}$	total
relative uncertainty	17.5%	9.7%	20.0%

TABLE I: Relative uncertainty budget for $I_3^E - I_3^R$ at $q_0 \simeq 0.1803 \Lambda = 0.152 \text{ GeV}/c$ from the dipole consideration.

The q_0 dependence is rather flat and in the interval at $\nu_0 = 0.15 - 0.3$ (that relates to $q_0 = (0.12 - 0.25) \text{ GeV}/c$) the value of $\delta I_3^E/I_3^E$ is not bigger than 25% (see Table II).

The uncertainty in I_3 at the level of 20% should affect the uncertainty of R_E from the Lamb shift in muonic hydrogen, but not dramatically.

q_0/Λ	q_0	$\delta I_{3<}^E/I_3^{\text{dip}}$	$\delta(I_{3>}^E - I_3^R)/I_3^{\text{dip}}$	total	<i>scatter</i>
0.10	0.084 GeV	9.7%	62%	63%	<i>11%</i>
0.15	0.126 GeV	14.6%	17.5%	22.3%	<i>5.5%</i>
0.20	0.169 GeV	19.4%	6.9%	20.6%	<i>3.0%</i>
0.25	0.211 GeV	24.2%	3.2%	24.4%	<i>1.7%</i>
0.30	0.253 GeV	29.1%	1.7%	29.2%	<i>0.9%</i>
0.40	0.337 GeV	38.8%	0.6%	38.8%	<i>0.3%</i>

TABLE II: Relative uncertainty budget for $I_3^E - I_3^R$ at various q_0/Λ from the dipole consideration. The last column is for the scatter in units of I^{dip} (see Sect. IV) It is shown in *italic* because it is not included into the error budget, but used to control the uncertainty.

IV. INTEGRATION OVER THE FITS

It would be indeed preferable to calculate $I_{3>}$ with real scattering data, which is unfortunately not that easy. Here, we use another opportunity and apply fits. However, we should distinguish a fit in an area, where we really have data, and a fit outside of such an area. The latter concerns not only the kinematic area, but also the accuracy. Indeed, we have certain data at low momentum transfer, but we have no direct data with sufficient accuracy for the subtracted form factor to calculate I_3 .

We intend to work with the fits in an area where all model-dependent effects are negligible. A reasonable estimation of the systematic uncertainty due to choice of the fits can be estimated by utilizing fits with consistent behavior at high and medium momentum transfer, but with different behavior at low momenta.

As an approximation, we apply fits for the electric form factor of the proton from Kelly, 2004 [9], Arrington and Sick, 2007 [10], Arrington et al., 2007 [11], Alberico et al., 2009 [12], Venkat et al., 2011 [13], and Bosted, 1995 [16].

Two of them are with so-called chain fractions, four fits are with Padé approximations with polynomials in q^2 and one is a Padé approximation with polynomials in q (see Appendix A).

The fits are quite close one to another and to the standard dipole parametrization in area of interest. Their comparison is presented in Fig. 4.

The low-momentum behavior of the fits is summarized in Table III. We see that the Padé fits tend to have a somewhat lower value of the radius and of the C coefficient, than those for the chain-fraction fits. All the radius values are substantially above the one from muonic hydrogen (see Fig. 1). The coefficient for the q^4 term for $(G_E(q^2))^2$ is quite above that for the standard dipole parametrization, but within the margins (1 ± 1), we have applied in our evaluation.

One of the fits (from [16]) is not included into Table III. That is a Padé approximation with polynomials in q (see

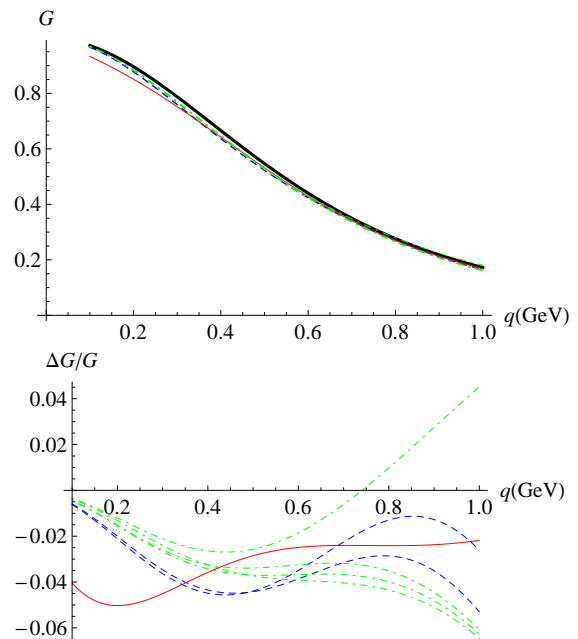


FIG. 4: The electric-charge form factor of the proton $G_E(q^2)$. Top: the dipole parametrization and the fits from [9–13, 16] (see Appendix A for details). Bottom: Relative deviation of the fits from the dipole form factor, $(G_E - G_{\text{dip}})/G_{\text{dip}}$. Horizontal axis: q [Gev/c]. Blue dashed lines are for the chain fractions, green dot-dashed lines are for Padé approximations with $\tau = q^2/4m_p^2$ and the red solid one is for the Padé approximation with q . The standard dipole approximation is presented with a black bold solid line in the top graph.

Eq. (A7)). Containing terms linear in q in the denominator, the fit definitely has a low-momentum behavior, strongly different from all the others. (Nothing is incorrect with the fit. It was designed as a phenomenological fit for not very low momentum transfer and is consistent there with the data.) Such an ‘inappropriate’ behavior of the fit makes it to be a perfect tool for tests on the model dependence related to the assumption on the low-momentum behavior.

The result of integration

$$I_{3>}^E - I_3^R = \int_{q_0}^{\infty} \frac{dq}{q^4} \left[(G(q^2))^2 - 1 \right]$$

over the different fits with the cut-off parameter $q_0 \simeq 0.1803 \Lambda = 0.152 \text{ GeV}/c$ lays from -25.8 GeV^{-3} to -24.5 GeV^{-3} (if we exclude integration over the fit with the Padé approximation in q) and from -29.6 GeV^{-3} (if we include it). For details, see Table IV.

We consider

$$I_{3>}^E - I_3^R = -25.2(6) \text{ GeV}^{-3}$$

as the estimation. The scatter of $I_3^E - I_3^R$ ($\pm 3.8\%$ if we exclude the fit with the Padé approximation in q) is below the total projected uncertainty and below the

fit	ref.	type	R_E [fm]	C [GeV $^{-4}$]
(A1)	[10]	chain fraction	0.90	34.3
(A2)	[10]	chain fraction	0.90	35.3
(A3)	[9]	Padé approximation (q^2)	0.86	28.0
(A4)	[11]	Padé approximation (q^2)	0.88	31.1
(A5)	[12]	Padé approximation (q^2)	0.87	28.2
(A6)	[13]	Padé approximation (q^2)	0.88	31.3

TABLE III: The low-momentum expansion of the fits for the electric form factor of the proton. The values are given for central values of the fits without any uncertainty. Here: $(G_E(q^2))^2 = 1 - R_E^2 q^2/3 + C q^4 + \dots$. The related values for the standard dipole fit are $R_E = 0.811$ fm and $C = 19.8$ GeV $^{-4}$. The spread of the central values of the charge radius (from 0.86 to 0.90 fm) is comparable with spread of central values of the results in Fig 1, which are 0.84 (μ H), 0.88 (H&D), 0.895 (Sick) and 0.88 (MAMI) fm.

fit	ref.	type	$I_{3>}^E - I_3^R$
(A1)	[10]	chain fraction	-25.7 GeV $^{-3}$
(A2)	[10]	chain fraction	-25.8 GeV $^{-3}$
(A3)	[9]	Padé approximation (q^2)	-24.5 GeV $^{-3}$
(A4)	[11]	Padé approximation (q^2)	-25.0 GeV $^{-3}$
(A5)	[12]	Padé approximation (q^2)	-24.7 GeV $^{-3}$
(A6)	[13]	Padé approximation (q^2)	-25.0 GeV $^{-3}$
(A7)	[16]	Padé approximation (q)	-29.6 GeV $^{-3}$

TABLE IV: Scatter of the results of numerical integration over the fits for $I_{3>}^E - I_3^R$ at ‘optimal’ $q_0 \simeq 0.1803 \Lambda = 0.152$ GeV/ c .

uncertainty for $I_{3>}^E - I_3^R$. Once we include the fit with the Padé approximation in q , the scatter becomes 14.8% which is comparable with the total uncertainty. Here, we show the scatter in various Tables, but do not include it into the error budget (see Table V). We denote the scatter without (A7) as *scatter* and the scatter with (A7) as *scatter**. We define the ‘scatter’ in the Tables as a half value of the difference between the maximal and minimal values. More discussion can be found in the conclusion section.

contribution	$\delta I_{3<}^E$	$\delta(I_{3>}^E - I_3^R)$	scatter	scatter*
dipole consideration	17.5%	9.7%		
integration over fits			3.8%	14.8%

TABLE V: The uncertainty and scatter for $I_{3>}^E - I_3^R$ at $q_0 \simeq 0.1803 \Lambda = 0.152$ GeV/ c .

We mentioned above that the fit (A7) from [16] has no reasonable behavior at low momentum. Nevertheless, its

use leads to a quite reasonable result which means that we are in a safe area of a model-independent application of the fits.

We remind that we have considered the $I_{3<}^E(\nu)$ in the previous section and the result for $\nu_0 = 0.1803$ gives

$$\begin{aligned} I_{3<}(\nu_0) &= 10(1 \pm \delta b) \frac{\nu_0}{\Lambda^3} \\ &= 3.0(3.0) \text{ GeV}^{-3}. \end{aligned} \quad (16)$$

Finally we obtain

$$I_3^E - I_3^R = -22.2(3.4) \text{ GeV}^{-3}.$$

The integral can be calculated for various q_0 (see, e.g., the results in Table VI). The result for $I_{3>}^E - I_3^R$ depends on q_0 , because the subtracted contribution (I_3^R) explicitly depends on q_0 . It is interesting to compare the scatter of $I_{3>}^E$ and the uncertainty. If we go to smaller values of q_0 , the variation of $G_E(q_0)$ from one fit to another becomes bigger than the uncertainty. For higher q_0 the scatter reduces and the fit (A7) with the Padé approximation in q [16] becomes more reasonable. The reduction of the scatter is due to the fact that the integrand for $I_{3>}$ is proportional $G_E^2 - 1$ and the contribution of the fit (i.e. of the G_E^2 term) becomes less and less important in comparison with the unity (see, e.g., Fig. 2), while the integral converges fast.

q_0/Λ	$I_{3>}^E - I_3^R$	scatter of $I_{3>}^E$	scatter* of $I_{3>}^E$
0.10	-57(11) GeV $^{-3}$	2.0 GeV $^{-3}$	18 GeV $^{-3}$
0.15	-30.8(3.9) GeV $^{-3}$	1.0 GeV $^{-3}$	5.0 GeV $^{-3}$
0.20	-18.0(3.5) GeV $^{-3}$	0.5 GeV $^{-3}$	1.7 GeV $^{-3}$
0.25	-10.4(4.2) GeV $^{-3}$	0.3 GeV $^{-3}$	0.6 GeV $^{-3}$
0.30	-5.4(5.0) GeV $^{-3}$	0.2 GeV $^{-3}$	0.2 GeV $^{-3}$
0.40	+0.9(6.7) GeV $^{-3}$	0.06 GeV $^{-3}$	0.06 GeV $^{-3}$

TABLE VI: Results for of $I_{3>}^E - I_3^R$ and its scatter from fit to fit at various values of q_0 .

V. THE EXTRACTION OF THE R_E VALUE FROM THE LAMB SHIFT

The purpose of this paper is not to obtain the proton charge radius from an *ab initio* analysis of the Lamb shift in muonic hydrogen, but to calculate the *shift* in the value of the proton radius due to a self-consistent treatment of the leading higher-order proton-finite-size contribution².

² Indeed, the I_3 contribution is only the leading proton-finite-size contribution beyond the R_E^2 term. There are additional smaller contributions, such as a recoil correction to the higher-order I_3 term, the proton-polarizability contribution etc. (see, e.g., [17]). They are in part included into the ‘QED’ term in (2).

The shift is in respect to already existing evaluations. Here, we first derive an expression for the shift of R_E and next discuss existing extractions.

We remind that the leading finite-nuclear-size contribution to the ns energy is

$$\frac{2}{3} \frac{(Z\alpha)^4}{n^3} m_r^3 R_E^2 \quad (17)$$

while the higher-order correction is

$$-\frac{16}{\pi} \frac{(Z\alpha)^5}{n^3} m_r^4 I_3^E. \quad (18)$$

For $l \neq 0$ both contributions are zero. For the application to measured transitions in muonic hydrogen [1, 2], $n = 2$.

Eq. (17) is not a complete result for the R_E^2 term, used in (1) and (2), because of an α -correction to the leading term (see, e.g., [8]). We deliberately ignore it here. The shift we are interested in, is not much affected by such a correction to the leading term and ignoring the correction we are well within uncertainty of our treatment for the shift.

After applying the self-consistent approach developed above, both finite-nuclear-size terms are effectively ‘renormalized’

$$\begin{aligned} \frac{2}{3} \frac{(Z\alpha)^4}{n^3} m_r^3 R_E^2 &\rightarrow \frac{2}{3} \frac{(Z\alpha)^4}{n^3} m_r^3 \left[1 - \frac{8(Z\alpha) m_r}{\pi q_0} \right] R_E^2, \\ -\frac{16}{\pi} \frac{(Z\alpha)^5}{n^3} m_r^4 I_3^E &\rightarrow -\frac{16}{\pi} \frac{(Z\alpha)^5}{n^3} m_r^4 (I_3^E - I_3^R), \end{aligned} \quad (19)$$

Denoting the ‘original’ values of R_E and I_3^E (from the existing evaluations) as R_E^0 and I_3^0 , we find

$$\begin{aligned} &\frac{2}{3} \frac{(Z\alpha)^4}{n^3} m_r^3 (R_E^0)^2 - \frac{16}{\pi} \frac{(Z\alpha)^5}{n^3} m_r^4 I_3^0 \\ &= \frac{2}{3} \frac{(Z\alpha)^4}{n^3} m_r^3 \left[1 - \frac{8(Z\alpha) m_r}{\pi q_0} \right] (R_E)^2 \\ &\quad - \frac{16}{\pi} \frac{(Z\alpha)^5}{n^3} m_r^4 (I_3^E - I_3^R). \end{aligned} \quad (20)$$

The combination in the left-hand-side of the identity is determined by a comparison of the experimental value with the ‘QED’ contribution in (1). Eventually we obtain

$$\begin{aligned} (R_E)^2 - (R_E^0)^2 &= \frac{1}{\left[1 - \frac{8(Z\alpha) m_r}{\pi q_0} \right]} \left[\frac{8(Z\alpha) m_r}{\pi q_0} (R_E^0)^2 \right. \\ &\quad \left. + \frac{24(Z\alpha) m_r I_3^0}{\pi} \frac{I_3^E - I_3^R - I_3^0}{I_3^0} \right]. \end{aligned} \quad (21)$$

To determine the shift, we have to consider, how I_3^0 was evaluated. We discuss below two CREMA’s publications³ [1, 2], where the most important extractions of

the proton charge radius were made and two different treatments of the integral under question have been applied. The results of our re-evaluation are summarized in Table VII.

ref.	R_E^0 [fm]	I_3^0 [GeV ⁻³]	$R_E - R_E^0$ [fm]	R_E [fm]
[1]	0.841 84(67)	19.25	-0.000 19(43)	0.841 65(79)
[2]	0.840 87(39)	22.9(1.2)	-0.000 65(43)(15)	0.840 22(56)

TABLE VII: Original parameters from CREMA’s extractions in [1] and [2] and the corrections to the charge radius due to the self-consistent evaluation of I_3^E . The uncertainties for the shift for the re-evaluation of the result from [2] are explained in the text.

Let us consider the previously applied evaluations in more detail. In case of the first extraction [1] of the proton radius from muonic hydrogen Lamb shift, the model for a calculation of the higher-order term suggested to apply a dipole shape of the form factor, but with an adjustable parameter. The parameter was linked to the radius. For more detail see, e.g., [8].

Technically, the result was

$$I_3^0 = \frac{105\pi}{32} \left(\frac{(R_E^0)^2}{12} \right)^{3/2}.$$

The result for the most optimal value ($q_0 \simeq 0.1803 \Lambda = 0.152 \text{ GeV}/c$) is

$$\begin{aligned} R_E &= 0.841 65(79) \text{ fm} \\ R_E - R_E^{\text{old}} &= -0.000 19(43) \text{ fm}, \end{aligned} \quad (22)$$

and the scatter due to choice of the fit is 0.000 08 fm. The extraction for various q_0 is presented in Table VIII.

q_0/Λ	R_E	$R_E - R_E^{\text{old}}$	scatter
0.10	0.841 34(150) fm	-0.000 49(135) fm	0.000 24 fm
0.15	0.841 59(83) fm	-0.000 25(49) fm	0.000 12 fm
0.20	0.841 68(80) fm	-0.000 16(44) fm	0.000 06 fm
0.25	0.841 73(85) fm	-0.000 11(52) fm	0.000 04 fm
0.30	0.841 76(91) fm	-0.000 08(62) fm	0.000 02 fm
0.40	0.841 80(106) fm	-0.000 04(82) fm	0.000 007 fm

TABLE VIII: The results for R_E at various values of q_0 as follows from (21). The scatter is related to the scatter of $I_{3>}^E$ in Table VI.

The results obtained at various q_0 are in a perfect agreement with each other and with (22) and all have comparable uncertainty, which is a strong confirmation of consistency of our method.

Above we have found a new value of the proton radius re-evaluating data from [1]. That is not the best one. A

³ We do not examine the extractions by themselves there. We consider only a shift due to change of the approach in treatment of I_3^E . Indeed, we understand that the results in Refs. [1, 2] are in part not compatible, because a more recent publication includes certain updates of theory.

better and somewhat more reliable result was published by the CREMA collaboration later in [2] on base of evaluation of their data from two $2s-2p$ transitions in muonic hydrogen. The QED theory was updated there as well as an evaluation of certain higher-order proton-structure effects was included. The original result of [2] is

$$R_E = 0.84087(39) \text{ fm} .$$

The uncertainty of 0.00031 fm comes from the experiment and 0.00029 fm is from theory, which, in particular, includes the uncertainties of the proton-polarizability and elastic-two-photon contributions (see Appendix B 2 for detail). The elastic two-photon contribution includes various recoil corrections, but the dominant part is still related to I_3^E , which involves some uncertainty due to a model-dependent evaluation of I_3^E . We have to find a new central value as explained above and to re-evaluate the uncertainty.

The results of re-evaluation of both CREMA's results are summarized in Table VII. The value of $R_E - R_E^0$ presented there has an uncertainty due to our re-evaluation of I_3^E , which is 0.00043 fm. It is the same for the re-evaluation of both CREMA's results. However, the later result has an uncertainty due to the evaluation of I_3^0 , which is 0.00015 fm. To check the consistency of the evaluation of I_3^E [17] used in [2] with ours, we have to combine the uncertainties, That leads to the overall uncertainty of 0.00045 fm. Meantime, to correct the radius, we have to remove the uncertainty of 0.00015 fm of the former evaluation and to include 0.00043 fm of ours.

Similarly to the consideration of the re-evaluation of the result from [1], we have calculated the result for the corrected radius for [2] at different values of the separation parameter q_0 . The results are summarized in Table IX. The results for the shift $R_E - R_E^{\text{old}}$ at various values of q_0 are consistent.

q_0/Λ	R_E	$R_E - R_E^{\text{old}}$	scatter
0.10	0.83990(140) fm	-0.00098(135)(15) fm	0.00024 fm
0.15	0.84015(62) fm	-0.00073(49)(15) fm	0.00012 fm
0.20	0.84025(59) fm	-0.00062(44)(15) fm	0.00006 fm
0.25	0.84030(65) fm	-0.00058(52)(15) fm	0.00004 fm
0.30	0.84033(73) fm	-0.00054(62)(15) fm	0.00002 fm
0.40	0.84037(91) fm	-0.00050(82)(15) fm	0.000007 fm

TABLE IX: The results for the correction to the charge radius of the proton at various values of q_0 for the extraction from [2] (cf. Table VIII).

VI. COMPARISON WITH FORMER EXTRACTIONS

Comparing the corrections we conclude that the model applied to the calculation of I_3 in the earlier CREMA

publication [1] happened to be somewhat more successful than the one applied later in [2]. Meantime, the latter model is more realistic. Let us briefly examine the correction in both cases and next explain why one description is somewhat more successful than the other.

The shift for the result from [1] is within the uncertainty of our calculations, which can be understood qualitatively.

Let us simplify the equation (21) for the correction. The first factor in the first term there deviates from unity only by a few percent and has been neglected in this section. We also explicitly split the original integral I_E^0 into three parts, corresponding to $I_{3<}^E, I_{3>}^E - I_3^R$ and I_3^R . The modified equation for the correction takes the form

$$\begin{aligned} (R_E)^2 - (R_E^0)^2 &\simeq \frac{24(Z\alpha)m_r}{\pi} \\ &\times \left\{ \int_0^{q_0} \frac{dq}{q^4} \left[\left((G_E(q^2))^2 - 1 - 2G'_E(0)q^2 \right) \right. \right. \\ &\quad \left. \left. - \left((G_0(q^2))^2 - 1 - 2G'_0(0)q^2 \right) \right] \right. \\ &\quad \left. + \int_{q_0}^{\infty} \frac{dq}{q^4} \left[(G_E(q^2))^2 - (G_0(q^2))^2 \right] \right. \\ &\quad \left. + \int_{q_0}^{\infty} \frac{dq}{q^2} \frac{R_E^2 - (\hat{R}_E^0)^2}{3} \right\} , \end{aligned} \quad (23)$$

where $G_0(q^2)$ is the form factor applied in the former evaluation and

$$(\hat{R}_E^0)^2 = -6G'_0(0)$$

is the radius, which follows from $G_0(q^2)$ and which does not necessarily coincide with R_E^0 .

The contribution from the low momenta is consistent with zero for both evaluations (in [1] and [2]) since the integral

$$\begin{aligned} &\int_0^{q_0} \frac{dq}{q^4} \left[\left((G_E(q^2))^2 - 1 - 2G'_E(0)q^2 \right) \right. \\ &\quad \left. - \left((G_0(q^2))^2 - 1 - 2G'_0(0)q^2 \right) \right] \\ &\simeq \left((1 \pm 1)C_{\text{dip}} - C_0 \right) q_0 \end{aligned}$$

agrees with zero within the uncertainty we applied. Here C_0 is the coefficient at q^4 for G_0 .

As for the data part

$$\int_{q_0}^{\infty} \frac{dq}{q^4} \left[(G_E(q^2))^2 - (G_0(q^2))^2 \right] ,$$

the situation in two former evaluations is different. In the case of the evaluation applied in [2], the fit used there is consistent with ours. The contribution of this term is consistent with zero and a departure from zero is below the uncertainty of our calculation.

Considering the evaluation of [1] *a posteriori*, the fit, which was used in there, is the dipole parametrization

with the parameter related to the final value of the charge radius. (Technically, they used the dipole fit with an adjustable parameter, but the parameter was determined by the extracted value of the radius.) For the contribution under question, a comparison of the standard dipole fit, which within a few percent is consistent with the fits we applied here, is plotted in Fig. 5. The discrepancy of the integrand for momenta above $q_0 \simeq 0.18 \Lambda = 0.15 \text{ GeV}/c$ is not more than 10%, which is the uncertainty of our calculation of $I_{3>}^E - I_3^R$. Thus the results for the correction should be still consistent with zero.

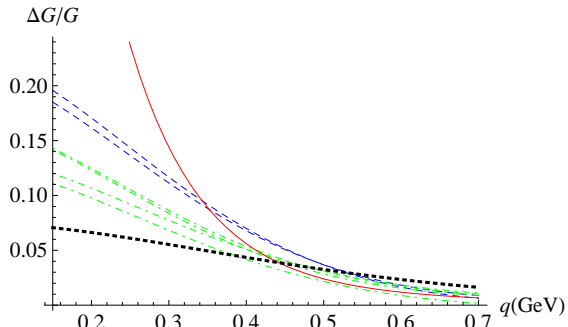


FIG. 5: Relative deviation of $(G_E^2 - 1)/q^4$, the integrand for $I_{3>}^E$, for the dipole fit with Λ , related to $R_E = 0.8418 \text{ fm}$ [1] (a bold black dotted line), from the standard dipole fit with $\Lambda^2 = 0.71 \text{ GeV}^2$. Effectively, the former fit was used in extraction in [1], while the latter dipole fit is better consistent with the data at high q . All the other lines are for the integrand from the fits used above and we use the same legend as in the previous plots.

The last term in (23) is

$$\int_{q_0}^{\infty} \frac{dq}{q^2} \frac{R_E^2 - (\hat{R}_E^0)^2}{3} = \frac{R_E^2 - (\hat{R}_E^0)^2}{3q_0}.$$

Since the evaluation in [1] is organized in such a way that the dipole fit has an adjustable parameter, we find

$$\hat{R}_E^0 = R_E^0 \simeq R_E.$$

In other words, neglecting a small correction to former radius, we see that the radius-related term for the shift is nearly vanishing. As a result, since two previous contributions are consistent with zero, the eventual shift of the re-evaluation of the result from [1] produces a shift in (22) which is within the uncertainty.

On the contrary, the radius-related term for the re-evaluation of the result from [2] does not vanish. It is not that small. While the radius extracted there is about the same as that extracted in [1], the fit applied for the evaluation of I_3^E assumed a value of $G'_E(0)$, which is not consistent with the radius. In other words, \hat{R}_E^0 was quite different there from R_E^0 of [2]. This produces a non-negligible contribution to the shift. Eventually, it

happens that the correction (23) for the shift from the result from [2] somewhat exceeds the uncertainty of our calculations.

It might look paradoxal and confusing that the correction for an evaluation with a rather unrealistic fit for the proton form factor is substantially smaller than the correction for an evaluation based on a ‘good’ fit of the data. However, one can see now that the effect was caused by the inconsistency of the applied fit (and the related charge radius from scattering [11]) and the value of the charge radius extracted from muonic hydrogen.

Roughly speaking there are two scenarios (without suggesting ‘new physics’) to explain the discrepancy between the results from the muonic-hydrogen Lamb shift and the electron-proton scattering.

- A). If the radius from the scattering is correct, that means that, since theory of muonic hydrogen is well established at the level of the controversy, the muonic-hydrogen experiment should be strongly incorrect. In this case there is not much sense to evaluate the I_3^E accurately.
- B). If the experiment on muonic hydrogen is correct (at the level of the discrepancy), then we have to conclude that the scattering result for the radius is wrong. The data are more or less correct. However, statistically evaluating a big set of the data, one may easily miss systematic effects which being negligible for each of data points, are important for their set as a whole. The accuracy of the fit in such a scenario should be overestimated.

One has to clearly distinguish between two kinds of fitting. A theoretically motivated fit with its shape known *a priori* is a way for the best determination of certain physical parameters and it allows afterwards any operations on the fit. On the contrary, a phenomenological fit does not determine any physical parameter, because the fit parameters may have no physical meaning at all. Such a fit is simply a function which is consistent with the data. Applying such a fit for interpolations, extrapolations and differentiations is, in general, questionable. As an example, we refer to the fits applied in our paper. The difference between the fit (A7) (with polynomials in q) from the other fits is within a few percent (as seen from Fig. 4), however behavior at low momentum is completely wrong and leads to an infinite value of the charge radius. Actually, considering a small term, linear in q , in any more reasonable fit would not break its consistency as far as such a term is small. But it should produce absolutely incorrect results for the charge radius and I_3^E . Indeed, we should exclude such a fit because it does not have an analytic behavior at low q^2 . So, the result strongly depends on theoretical constraints accompanying the fitting procedure. However, there is no reason to expect that just limiting considerations to analytic functions at low q^2 is sufficient to

obtain a correct extrapolation at low momentum. There may be other important constraints which may affect the final results. As we mentioned in the introduction, there is no fit which is literally correct and is consistent with all the data.

The missed systematic effects can be in the raw data, in their theoretical evaluation (by correcting for QED effects and proton polarizability) or just in fitting with an arbitrary class of functions, which by the way does not reproduce⁴ correct analytic behavior at negative q^2 .

In this scenario, while the data are roughly correct, the very shape of the fit is much more uncertain than expected. The value of $G'_E(0)$ should be linked to the charge radius whatever it is. In this scenario, such a radius is to be from muonic hydrogen.

That means that the difference in results for the complete integral I_3^E between different evaluations (23) is basically due to appropriate (or non-appropriate) choice of $G'_E(0)$. The unrealistic fit (the dipole parametrization with the parameter to be consistent with the final value of the charge radius as in [1]) for the subtracted form factor has reasonable behavior at relatively large q^2 , while the realistic fit for the subtracted form factor, which produces a higher value of R_E , has ‘bad’ behavior at high q^2 . The ‘direct’ data contribution is relatively unimportant in this area as seen in Fig 2.

That explains, why the correction is bigger for the re-evaluation of the more recent CREMA’s result from [2], than for the re-evaluation of the result from [1].

Concluding the discussion on the central value of the correction, we have to stress that the uncertainty of the correction does not depend too much on the choice of the model to evaluate the higher-order proton-finite-size contribution. We strongly believe that the uncertainty of this term was underestimated in the past.

VII. CONCLUSIONS

Above, we have re-evaluated the contribution of I_3^E only. All other details have not been reconsidered. The final value of the proton charge radius should be obtained from the re-evaluation of the more recent CREMA publication [2], which has certain advantages from the experimental and theoretical point of view.

⁴ One should not overestimate this issue. The hadronic vacuum polarization in the two-pion channel can be considered in different ways. A well-known ‘realistic’ form factor of the pion by Gounaris and Sakurai [19] allows to take into account the correct position of the branch point and the cut line for two-pion production, however, the eventual result for the vacuum polarization operator at space-like momentum is not much different from a bold picture with just a narrow ρ -meson pole.

The new value of the radius obtained here is

$$R_E = 0.840\,22(56)\text{ fm}.$$

The uncertainty is bigger than in the original publication [2].

The scatter in the calculations of $I_>$ is comparable with our estimation for the uncertainty and it is rather smaller than our estimation of $\delta I_{3>}^E$ (if we exclude (A7)). Including the fit (A7) with inappropriate behavior at low q , we increase the scatter, but not too much. Behavior of various fits in the region suitable for the choice of the separation parameter q_0 is presented in Fig. 6.

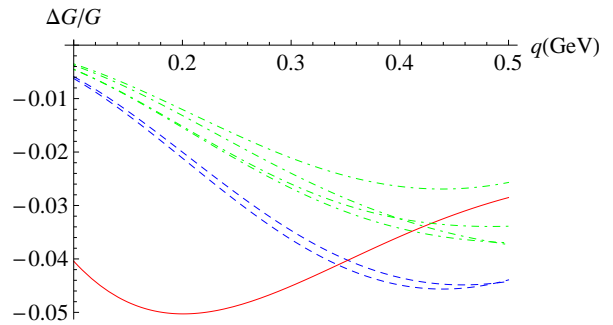


FIG. 6: Relative deviation of the electric form factor from the dipole form factor $(G_E - G_{\text{dip}})/G_{\text{dip}}$. The horizontal axis: q [Gev/c].

Our estimation of the uncertainty is arbitrary to a certain extent, but seems reasonable. The estimation of the uncertainty of the form factor at q_0 as 1% is validated by the behavior of the fits and the obtained scatter of the results. Nevertheless, a direct examination of the experimental data around potential values of q_0 , a verification of their uncertainty and, if possible, its improvement below the level of 1% would be appreciated.

The same could be concluded about an estimation of the q^4 term as within a possible 100% deviation from the dipole value. It is validated by the scatter of the results of various fits applied here. It is consistent with fits considered by MAMI [4] (see [20] for details.) as well. Such an estimation also has sense if one recalls a geometrical meaning of the form factor at low q^2 . Due to that one may expect that its behavior is basically determined by a single parameter, namely the characteristic size of the proton, which is a quite compact object.

The situation may look somewhat similar to that for the anomalous magnetic moment of muon. Any precision QED calculations are incomplete and at certain stage one has to deal with hadronic effects. In particular, in case of $g - 2$ of the muon and the hyperfine interval in muonium the hadronic contributions are presented with the hadronic vacuum polarization. One may think that dealing with the proton form factor while calculating the energy levels in muonic hydrogen is similar to the treatment of the hadronic vacuum polarization effects. However,

this impression is incorrect. Integration for the hadronic vacuum polarization is done [21, 22] directly over the data with no subtractions or extrapolations. That makes such evaluations reliable. The involvement of the subtractions and extrapolations in case of the higher-order proton-finite-size corrections has changed the situation completely and requires a different considerations, which is presented in this paper.

The author is grateful to S. Eidelman and V. Ivanov for useful discussions. This work was supported in part by DFG under grant HA 1457/9-1.

Appendix A: Fits for the electric form factor of the proton applied in the paper

The fits for G_E applied in the paper include two chain-fraction fits. Both are from Arrington and Sick, 2007, [10]. The first one is completely based on [10]⁵

$$G_E(q^2) = \frac{1}{1 + \frac{3.44Q^2}{1 - \frac{0.178Q^2}{1 - \frac{1.212Q^2}{1 + \frac{1.176Q^2}{1 - 0.284Q^2}}}}}, \quad (\text{A1})$$

while the other is obtained in [10] by applying the two-photon correction according to [23]

$$G_E(q^2) = \frac{1}{1 + \frac{3.478Q^2}{1 - \frac{0.140Q^2}{1 - \frac{1.311Q^2}{1 + \frac{1.128Q^2}{1 - 0.233Q^2}}}}}. \quad (\text{A2})$$

Four fits are with the Padé approximation in q^2 , originally introduced by Kelly, 2004, [9]

$$G_E = \frac{1 - 0.24\tau}{1 + 10.98\tau + 12.82\tau^2 + 0.863\tau^3}, \quad (\text{A3})$$

where

$$\tau = q^2/4m_p^2,$$

and later developed by Arrington et al., 2007, [11]

$$G_E = \frac{1 + 3.439\tau - 1.602\tau^2 + 0.068\tau^3}{D_A}, \quad (\text{A4})$$

$$D_A = 1 + 15.055\tau + 48.061\tau^2 + 99.304\tau^3 + 0.012\tau^4 + 8.650\tau^5,$$

Alberico et al., 2009, [12]

$$G_E(q^2) = \frac{1 - 0.19\tau}{1 + 11.12\tau + 15.16\tau^2 + 21.25\tau^3}, \quad (\text{A5})$$

⁵ Here, Q is the numerical value for the momentum transfer q in GeV.

and Venkat et al., 2011, [13]

$$G_E = \frac{N_V}{D_V},$$

$$N_V = 1 + 2.90966\tau - 1.11542229\tau^2 + 3.866171 \times 10^{-2}\tau^3$$

$$D_V = 1 + 14.5187212\tau + 40.88333\tau^2 + 99.999998\tau^3 + 4.579 \times 10^{-5}\tau^4 + 10.3580447\tau^5. \quad (\text{A6})$$

One more fit with is the Padé approximation in q from Bosted, 1995, [16]

$$G_E(q^2) = \frac{1}{1 + 0.62Q + 0.68Q^2 + 2.8Q^3 + 0.83Q^4}. \quad (\text{A7})$$

Appendix B: Evaluation of I_3^E in former extractions of R_E from the Lamb shift in muonic hydrogen

1. Evaluation in [1]

The calculation of I_3^E in [1] was done by applying the dipole parametrization with a free parameter and allowing this parameter to be consistent with the radius extracted (see, e.g., [8]).

2. Evaluation in [2]

The result for the evaluation of I_3^E , applied in [2], was not presented there directly, being a part of the adopted there value for the two-photon-exchange correction. The result for the two-photon-exchange was taken from [18]. That result is a sum of ‘elastic’ and polarizability contributions, with the former strongly dominating. Meanwhile, the ‘elastic’ term was not calculated there, but taken from [17]. Their calculation of the ‘elastic’ term takes into account recoil effects. Nevertheless, the leading contribution is a non-recoil one, which is determined by I_3^E . The value of integral was found by integrating over the fit (A4) from [11]. The uncertainty was estimated via a comparison with results from some other fits, such as (A3) [9].

Thus, the leading model-dependent effect due to the form factors is still from the calculation of I_3^E , the central value of which was obtained by applying (A4).

[1] R. Pohl, A. Antognini, F. Nez, F.D. Amaro, F. Biraben, J.M.R. Cardoso, D.S. Covita, A. Dax, S. Dhawan, L.M.P.

Fernandes, A. Giesen, T. Graf, T.W. Hänsch, P. Indeli-

- cato, L. Julien, Cheng-Yang Kao, P. Knowles, E.-O. Le Bigot, Yi-Wei Liu, J.A.M. Lopes, L. Ludhova, C.M.B. Monteiro, F. Mulhauser, T. Nebel, P. Rabinowitz, J.M.F. dos Santos, L.A. Schaller, K. Schuhmann, C. Schwob, D. Taqqu, J.F.C.A. Veloso and F. Kottmann, *Nature (London)* **466**, 213 (2010).
- [2] A. Antognini, F. Nez, K. Schuhmann, F.D. Amaro, F. Biraben, J.M.R. Cardoso, D.S. Covita, A. Dax, S. Dhawan, M. Diepold, L.M.P. Fernandes, A. Giesen, A.L. Gouvea, T. Graf, T.W. Hänsch, P. Indelicato, L. Julien, Cheng-Yang Kao, P. Knowles, F. Kottmann, E.-O. Le Bigot, Yi-Wei Liu, J.A.M. Lopes, L. Ludhova, C.M.B. Monteiro, F. Mulhauser, T. Nebel, P. Rabinowitz, J.M.F. dos Santos, L.A. Schaller, C. Schwob, D. Taqqu, J.F.C.A. Veloso, J. Vogelsang, R. Pohl, *Science*, **339** 417 (2013).
- [3] I. Sick, *Phys. Lett. B* **576**, 62 (2003).
- [4] J.C. Bernauer, P. Achenbach, C. Ayerbe Gayoso, R. Böhm, D. Bosnar, L. Debenjak, M.O. Distler, L. Doria, A. Esser, H. Fonvieille, J.M. Friedrich, J. Friedrich, M. Gómez Rodríguez de la Paz, M. Makek, H. Merkel, D.G. Middleton, U. Müller, L. Nungesser, J. Pochodzalla, M. Potokar, S. Sánchez Majos, B.S. Schlimme, S. Širca, Th. Walcher, and M. Weinriefer, *Phys. Rev. Lett.* **105**, 242001 (2010).
- [5] P.J. Mohr, B.N. Taylor, and D.B. Newell, *Rev. Mod. Phys.* **84**, 1527 (2012).
- [6] S.G. Karshenboim, *Annalen der Physik* **525**, 472 (2013).
- [7] S.G. Karshenboim, *Physics-Uspekhi* **56**, 883 (2013).
- [8] M.I. Eides, H. Grotch, and V.A. Shelyuto, *Theory of Light Hydrogenic Bound States*, Springer Tracts Mod. Phys. **222** (Springer, Berlin, Heidelberg, 2007).
- [9] J.J. Kelly, *Phys. Rev. C* **70**, 068202 (2004).
- [10] J. Arrington and I. Sick, *Phys. Rev.* **C76**, 035201 (2007).
- [11] J. Arrington, W. Melnitchouk, and J.A. Tjon, *Phys. Rev.* **C76**, 035205 (2007).
- [12] W.M. Alberico, S.M. Bilenky, C. Guinti, and K.M. Graczyk, *Phys. Rev.* **C79**, 065204 (2009).
- [13] S. Venkat, J. Arrington, G.A. Miller and X. Zhan, *Phys. Rev.* **C83**, 015203 (2011).
- [14] I.T. Lorenz, H.W. Hammer, U.G. Meissner, *Eur. Phys. J.* **A48**, 151 (2012).
- [15] S.G. Karshenboim, *Phys. Lett.* **A225**, 97 (1997).
- [16] P.E. Bosted, *Phys. Rev.* **C51**, 409 (1995).
- [17] C.E. Carlson and M. Vanderhaeghen, *Phys. Rev.* **A84**, 020102 (2011).
- [18] M.C. Birse and J.A. McGovern, *Eur. Phys. J.* **A48**, 120 (2012).
- [19] G.I. Gounaris and J.J. Sakurai, *Phys. Rev. Lett.* **21** 244 (1968).
- [20] J. Bernauer, *Measurement of the elastic electron-proton cross section and separation of the electric and magnetic form factor in the Q^2 range from 0.004 to 1 $(\text{GeV}/c)^2$* . Ph.D. Thesis, Mainz, 2010. Available at <http://www1.kph.uni-mainz.de/A1/publications/doctor/bernauer.p>
- [21] F. Jegerlehner, *The Anomalous Magnetic Moment of the Muon*. Springer, Berlin and Heidelberg: Springer Tracts in Modern Physics **226** (2007).
- [22] A. Czarnecki, S. I. Eidelman and S. G. Karshenboim, *Phys. Rev.* **D65** (2002).
- [23] P.G. Blunden, W. Melnitchouk, and J.A. Tjon, *Phys. Rev.* **C72**, 034612 (2005).